Atmos. Chem. Phys. Discuss., https://doi.org/10.5194/acp-2018-121
Manuscript under review for journal Atmos. Chem. Phys.
Discussion started: 6 April 2018
© Author(s) 2018. CC BY 4.0 License.

Atmospheric Chemistry and Physics
Discussions

Intermittent turbulence contributes to vertical diffusion of $PM_{2.5}$ in the North China Plain

Wei Wei[1], Hongsheng Zhang[2], Bingui Wu[3], Yongxiang Huang[4], Xuhui Cai[5], Yu Song[5], Jianduo Li[1]

[1]State Key Laboratory of Severe Weather, Chinese Academy of Meteorological Sciences, Beijing 100081, P.R. China
[2]Laboratory for Climate and Ocean-Atmosphere Studies, Department of Atmospheric and Oceanic Sciences, School of Physics, Peking University, Beijing 100081, P.R. China
[3]Tianjin Municipal Meteorological Bureau, Tianjin 300074, P.R. China
[4]State Key Laboratory of Marine Environmental Science, Xiamen University, Xiamen 361005, P.R. China
[5]State Key Joint Laboratory of Environmental Simulation and Pollution Control, Department of Environmental Science, Peking University, Beijing 100081, P.R. China

Correspondence to: Hongsheng Zhang (hsdq@pku.edu.cn)

Abstract. Heavy particulate pollution events have frequently occurred in the North China Plain over the past decades. Due to high emissions and poor diffusion conditions, issues become increasingly serious during cold seasons. Although early studies have explored some potential reasons for air pollutions, there are few works focusing on the effects of intermittent turbulence. This paper draws upon two typical $PM_{2.5}$ (particulate matters with diameter less than 2.5 mm) pollution cases from the winter of 2016–2017. After several days of gradual accumulation, the concentration of $PM_{2.5}$ near the surface reached the maximum as a combined result of strong inversion layer, stagnant wind and high ambient humidity and then sharply decreased to a very low level within a few hours. In order to identify the strength of turbulent intermittency, an effective index, called Intermittency Factor (IF), was proposed by this work. The results show that the turbulence during the stage of diffusion is highly intermittent and not locally generated. The vertical characteristics of IF and wind filed confirm the generation and downward transport of intermittent turbulence from the wind shear associated with low-level jets. The intermittently turbulent fluxes contribute positively to the vertical dispersion of particulate matters and improve the air quality near the surface. This work brought up a possible mechanism of how intermittent turbulence affects the diffusion of particulate matters.

1 Introduction

In the winter of 2016–2017, severe air pollution events haunted the North China Plain, affecting more than 1/5 of the total population in China (Ren et al., 2017). Particulate pollution, especially $PM_{2.5}$ (particulate matters with diameter less than 2.5 mm) pollution, has become the foremost problem, considering its adverse impacts on human health (Dominici et al., 2014; Nel, 2005; Thompson et al., 2014; Zheng et al., 2015b).

Naturally, researchers are alarmed by these issues and want to understand the potential reasons. Some works (Wang et al., 2010; Zhang et al., 2016) reveal the effects of the increasing consumption of fossil fuel and the production of secondary pollutants. Meanwhile, it is reported that climate change (Yin et al., 2017; Yin and Wang, 2017) and synoptic circulation (Miao et al., 2017; Ye et al., 2016; Zhang et al., 2012; Zheng et al., 2015a) are of great importance in the transport of pollutants as well. Air pollution is essentially a phenomenon of the atmospheric boundary layer (ABL) and is strongly affected by the thermodynamic and dynamic structure of the ABL (Bressi et al., 2013; Gao et al., 2016; Tang et al., 2016). The spatial and temporal structures of turbulent motions have a dominant influence on the local air quality from the hourly scale to the diurnal scale (Shen et al., 2017). However, most of the works (Petäjä et al., 2016) focus on the feedback between aerosol, turbulent mixing and boundary layer, with little discussion on the dynamic effect of turbulence on the transport of particulate matters, not to mention the intermittent turbulence under strongly stable conditions. In fact, severe particulate pollutions tend to frequently occur in cold seasons in northern China (Sun et al., 2004; Zhang and Cao, 2015), during which the stratification of the ABL is more stable (Wang et al., 2017) and the turbulent mixing is relatively weak and intermittent in both temporal and spatial scales (Klipp and Mahrt, 2004; Mahrt, 2014). A series of works (Helgason and Pomeroy, 2012; Noone et al., 2013; Vindel and Yagüe, 2011) have confirmed that the intermittent turbulence accounts for a large amount of the vertical momentum, heat and mass exchange between the surface and the upper boundary layer, implying that intermittent turbulence may be one of the key factors in the pollutant dispersion.

The intermittency of velocity fluctuations comes in bursts (as shown in Figure 2 in Frisch, 1980), which means that turbulent intermittency is non-stationary and has no specific time scale. Moreover, the turbulence in the ABL is inherently nonlinear (Holtslag, 2015) and has complex interaction with other motions, such as low-level jets, gravity waves, solitary waves and other non-turbulence motions (Banta et al., 2006; Sun et al., 2015; Terradellas et al., 2005). To date, different methods have been applied to describe the levels of intermittency, such as the flatness (Frisch, 1995), FI index (Mahrt, 1998), wavelet analysis (Salmond, 2005) and so on. Given the non-linearity and non-stationarity of intermittent turbulence in the ABL, we conduct our study using a new technique, the so-called arbitrary-order Hilbert spectral analysis (arbitrary-order HSA, Huang et al., 2008), which has been successfully applied into the analyses of turbulence (Huang et al., 2009, 2011; Schmitt et al., 2009; Wei et al., 2016, 2017). It should be noticed that, the target of this work is not to compare the cons and pros of different methods but to study the turbulent intermittency in the ABL with the help of an effective method. The methodology is generalized and the advances are clarified in Sect. 2.2.

Based on these considerations, this work mainly aims at:

1) quantifying the turbulent intermittency in the ABL using the arbitrary-order HSA technique;
2) revealing a possible mechanism of the diffusion of near-surface $PM_{2.5}$ from a viewpoint of intermittent turbulence.

In the following text, the data and method are introduced in Sect. 2, respectively. Then Sect. 3 discusses our results in detail, including an overview of the cases, the behavior of turbulence intermittency and its contribution to the pollutant transport. The last Sect. 4 is a conclusion.

2 Data and Method

2.1 Observation

Tianjin (39.00 °N, 117.21°E, altitude 3.4 m) is the largest coastal city in the North China Plain with a population of more than 1.5 million, covering an area of 11,300 km^2. Tianjin is located to the east of Beijing, the capital of China, and neighbors Bohai Sea to the east (Fig. 1). Due to the rapid urbanization in the past decades, Tianjin has a typical urban underlying terrain.

Observations in this work include three parts: 1) a 255-m meteorological observation tower for the measurement of turbulence; 2) a CFL-03 wind-profile radar (WPR) for the boundary-layer wind field; and 3) a TEOM 1405-DF system for the monitor of particular matters. The 255-m meteorological observation tower is situated in the Tianjin Municipal Meteorological Bureau, equipped with three levels (40, 120, and 200 m) of sonic anemometers (CSAT, CAMPBELL, Sci., USA) operating at a sampling frequency of 10 Hz. In addition, the observation by HMP45C probe (CAMPBELL, Sci., USA) at 15 levels is also used to analyze the behavior of relative humidity (RH) and temperature. The Tianjin Municipal Meteorological Bureau is located in a residential and traffic area and the buildings around the 255-m meteorological observation tower are typically 15-25 m in height (Ye et al., 2014). In order to avoid affecting the residential zone, the CFL-03 boundary-layer WPR is mounted nearly 10 km away from the Tianjin Municipal Meteorological Bureau to the west. The 1405-DF TEOM system is installed at a height of 3 m to monitor the surface PM$_{2.5}$. Detailed information is listed in Table 1.

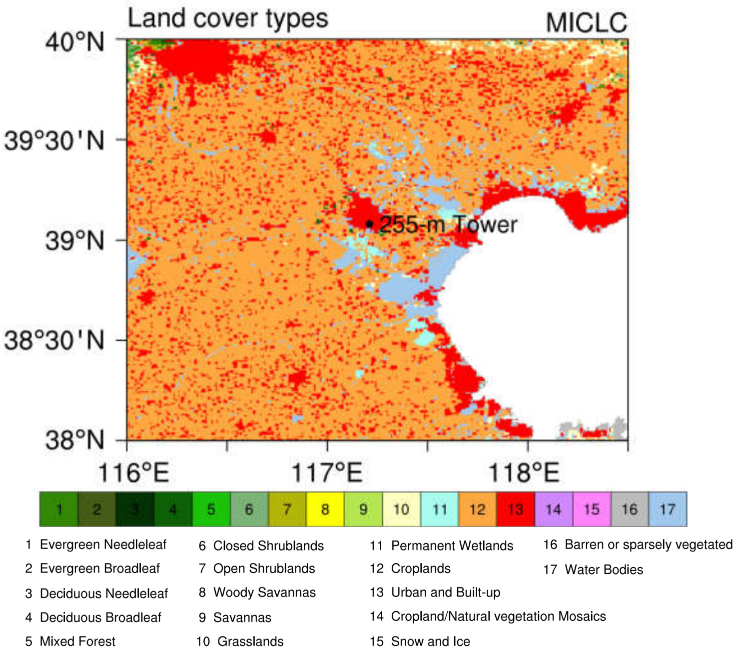

Figure 1: Landuse map around the site. The black dot denotes the location of the 255-m meteorological observation tower.

Table 1. Performance characteristics of instruments

Instrument	Height	Variables	Sampling resolution	Range	Accuracy
Sonic anemometer-thermometer, CSAT3[a]	40, 120, 200 m	3-D wind speed Sonic virtual temperature	0.1 s	u_x, u_y: ± 65.536 m s^{-1} u_z: ± 8.192 m s^{-1} c: 300–366 m s^{-1} (-50–60°C)	u_x, u_y: < ± 4 cm s^{-1} u_z: < ± 2 cm s^{-1}
HMP45C[a]	15 levels[b]	Temperature, Relative humidity	15 s	-40–60°C 0–100%	± 0.2°C ± 2% (<90%) ± 3% (>90%)
1405-DF TEOM[c]	3 m	$PM_{2.5}$	1 hr	0–1,000,000 μg m^{-3}	± 7.5%
CFL-03 boundary layer WPR[d]	< 5,000 m	Horizontal/vertical wind speed ($U_{h/v}$), wind direction	Temporal: 10 min Vertical: 100 m	U_h: 0–60 m s^{-1} U_v: ±20 m s^{-1} Direction: 0–360°	$U_{h/v}$: 0.1 m s^{-1} Direction: ≤ 10°

[a] CAMPBELL, Sci., USA
[b] 15 levels: 5, 10, 20, 30, 40, 60, 80, 100, 120, 140, 160, 180, 200, 220, and 250 m
[c] Thermo Fisher Scientific, USA
[d] China Aerospace Science & Industry Corp

Turbulence observations from the 255-m tower were obtained at a sampling frequency of 10 Hz. Then quality control was applied to all the data (Zhang et al., 2001), such as error flag, spike detection, cross wind correction, spectral loss correction, sonic virtual temperature correction, density fluctuation correction, and coordinate rotation. An averaging time length of 1 min was applied to calculate turbulent fluctuations and fluxes, given the small size eddies under stable conditions. The friction velocity u_* reads in its form as $u_* = (\overline{u'w'}^2 + \overline{v'w'^2})^{1/4}$, where $\mathrm{u}'/\mathrm{v}'/\mathrm{w}'$ represent the longitude, lateral and vertical fluctuation of wind vector. The turbulent kinetic energy (TKE) is given by $\mathrm{TKE} = (\overline{u'}^2 + \overline{v'}^2 + \overline{w'^2})/2$ and the stability function uses $\mathrm{z/L} = -\kappa z g \overline{w'\theta'}/\bar{\theta}u_*^3$, in which $\mathrm{L} = -\bar{\theta}u_*^3/\kappa g \overline{w'\theta'}$ is Obukhov length, θ is potential temperature and κ is von Karman constant with a value of 0.4 here. The data quality of CFL-03 boundary-layer WPR was checked to avoid the effects of poor data. First, data below 200 m were removed due to the interference of surrounding environment, including trees and buildings. Then each vertical profile was checked through and points with larger than 2.5 standard deviations were regarded as outliers and discarded.

Based on an overall consideration of data quality and severity of air quality, two cases happening in the winter of 2016–2017 were identified to study the relationship between intermittent turbulence and pollutant dispersion. The first one persisted for 5 days from 00:00 on 23 November 2016 to 00:00 on 28 November 2016, which is marked as Case-1 for convenience purposes. The second case, that is, Case-2, is from 00:00 on 23 January 2017 to 00:00 on 30 January 2017. All of the time in this work refers to local standard time.

2.2 Method

The flow in the ABL is highly nonlinear and non-stationary. In order to deal with the nonlinear and non-stationary time series, we adopted a relatively new technique called the arbitrary-order Hilbert spectral analysis (arbitrary-order HSA, Huang et al., 2008), which is based on the Hilbert-Huang transform (Huang et al., 1998, 1999). The primary reason why the arbitrary-order HSA is used in this work is that this method satisfies locality and adaptivity which are two necessary conditions for the study of nonlinear and non-stationary time series (Huang et al., 1998). On this basis, we proposed an index, called intermittent factor (IF), to quantify the level of turbulent intermittency. To investigate the effects of vertical mixing in the diffusion of air pollutants, a set of vertical wind fluctuation at 10 Hz obtained by the sonic anemometers (CSAT3, CAMPBELL Inc., USA) were drawn upon in this study. A brief introduction to the method is mathematically described in this part. For detailed information, one can refer to the work by Huang et al. (2008).

Firstly, a 30-min vertical wind-speed signal X(t) is separated into a group of intrinsic mode functions $C_i(t)$ and a residual $r_n(t)$ according to the so-called empirical mode decomposition. Here, each intrinsic mode functions $C_i(t)$ meets two constraints: (i) the difference between the number of local extrema and the number of zero-crossings must be zero or one, and (ii) the running mean values of upper and lower envelops are zero. The decomposition process is as follows (Huang et al., 1998, 1999):

1) The first step is to form the upper envelope $e_{max}(t)$ based on the local maxima of X(t) using the cubic spline interpolation. The lower envelope $e_{min}(t)$ can be constructed following the same method.
2) Then, one can define the mean $m_1(t) = (e_{max}(t) + e_{min}(t))/2$ and the first local signal $h_1(t) = X(t) - m_1(t)$.
3) So far, $h_1(t)$ is checked whether it meets the two constraints of intrinsic mode functions. If yes, $h_1(t)$ is the first intrinsic mode function $C_1(t) = h_1(t)$ and is taken away from X(t) to obtain the first residual $r_1(t) = \mathrm{X(t)} - C_1(t)$. Then $r_1(t)$ is treated as the new signal to begin with step 1). If $h_1(t)$ does not meet the above constraints, the first step is repeated on $h_1(t)$ to define the lower and upper envelopes and further the new local detail until $h_{1k}(t)$ is the first intrinsic mode function $C_1(t) = h_{1\mathrm{k}}(t)$.

Steps 1–3 are called ‘sifting process’. To avoid over-sifting, the standard deviation criterion (Huang et al., 1998) is applied to stop this decomposition process. After n times of ‘sifting process’, one obtains a set of $C_i(t)$ and a monotonic residual $r_n(t)$. At this point, the vertical wind fluctuation X(t) can be expressed as $\mathrm{X(t)} = \sum_{i=1}^{n} C_i(t) + r_n(t)$. Then, each mode $C_i(t)$ is developed to obtain its corresponding analytical signal $C_i^A(\mathrm{t}) = C_i(t) + j\tilde{C}_i(t) = A_i(t)\exp(j\theta_i(t))$using Hilbert transform (Cohen, 1995), where the imaginary part reads as $\tilde{C}_i(t) = \frac{1}{\pi}\int_{-\infty}^{\infty}\frac{C_i(\tau)}{t-\tau}d\tau\frac{d\theta_i}{dt}$, and $A_i(t)$ and $\theta_i(t)$ are the instantaneous amplitude and phase. Also, one can define the instantaneous frequency as $\omega_i(t) = \frac{1}{2\pi}\frac{d\theta_i}{dt}$.

Note that the instantaneous amplitude $A_i(t)$ and frequency $\omega_i(t)$ are both a function of time, which means that a Hilbert spectrum $\mathrm{H}(\omega, t)$ can be defined with $A_i(t)$ expressed in the space of frequency–time. So does the joint probability density function (p.d.f.) $\mathrm{p}(\omega, A)$. Then $\mathrm{H}(\omega, t)$ can be further expressed as $\mathrm{H}(\omega) = \int \mathrm{p}(\omega, A) A^2 dA$. If the power exponent of instantaneous amplitude is extended from 2 to q, one can define arbitrary-order Hilbert spectrum as $\mathcal{L}_q(\omega) = \int \mathrm{p}(\omega, A) A^q dA$, where $\mathrm{q} \geq 0$ is the arbitrary moment.

In the case of scale invariance, the arbitrary-order Hilbert spectrum follows $\mathcal{L}_q(\omega) \sim \omega^{-\xi(q)}$ in the inertial subrange, in which ω is the frequency and $\xi(q)$ is the scaling exponent function. Under the assumption of fully developed turbulence, the distribution of scaling exponent function with the order q is linear and meets $\xi(q) - 1 = q/3$, which is developed from $\xi(q) = \zeta(q) + 1$ (Huang et al., 2008, 2011), where $\zeta(q)$ is the scaling exponent function in q–order structure function $S_q(l) = \langle(\delta X(l))^q\rangle = \langle(X(l + l_0) - X(l_0))^q\rangle \sim l^{\zeta(q)}$, in which the angular bracket refers to spatial averaging and l means distance. This exponent law is in agreement with Kolmogorov's hypothesis (K41 for short) and any intermittency would result in deviations from the theoretical $q/3$ (Basu et al., 2004). Based on this, we define an index, called Intermittent Factor (IF), as the deviation from the theoretical value at the maximal order: $\mathrm{IF} = \xi(q_{max}) - 1 - q_{max}/3$. Due to the limited observation length, the maximal order q_{max} is up to 4 in this study to avoid the difficulties and errors in the measurements of high-order moments (Frisch, 1995).

It is well acknowledged that the intermittent turbulence under stable conditions is characterized by sporadic bursts in a timescale of order $\mathrm{O}(10)$ to $\mathrm{O}(1000)$ sec. The statistically unsteady turbulence disobeys the assumptions of traditional theories (Poulos et al., 2002). For example, Fourier spectral analysis asks for a linear system and strictly stationary data; and the widely used wavelet transform is suitable for non-stationary signals but suffers when it comes to nonlinear cases (Huang et al., 1998). As one of the most important steps through this method, the empirical mode decomposition separates the original time series into different modes based on its own physical characteristics without any predetermined basis. And with the instantaneous information from the Hilbert transform, one can investigate the behavior of local events, which makes the Hilbert-based method more appropriate for the analyses of intermittent turbulence. This Hilbert-based scaling exponent function $\xi(q)$ has been applied into the analyses of turbulent intermittency in the ABL (Wei et al., 2016, 2017) and shown its effectiveness and validity.

3 Results and Discussion

3.1 Overview of Cases

Figure 2 illustrates the time series of different variables for two cases, including surface $PM_{2.5}$ concentration, wind vector, temperature, RH, horizontal wind speed, vertical wind speed, friction velocity u_*, TKE, and stability parameter $\mathrm{z/L}$. From the distribution of $PM_{2.5}$, it can be seen that the concentration of pollutants gradually increased to a maximum of 412 μg m^{-3}

© Author(s) 2018. CC BY 4.0 License.

for $PM_{2.5}$ and then dropped to a low level within a few hours no matter for Case-1 and Case-2. Based on the concentration of $PM_{2.5}$, we can easily divide each case into two periods: one called the cumulative stage (CS) during which particulate matters accumulate near the surface; the other named as the transport stage (TS) representing the stage when pollutants dissipate (Zhong et al., 2017). At this point, Case-1 can be separated into the CS from 00:00 on 23 Nov to 06:00 on 27 Nov 2016 and the TS from 06:00 on 27 Nov to 00:00 on 28 Nov 2016. Case-2 experienced two transitions from the CS to TS which happened at 00:00 on 26 January 2017 and at 00:00 on 29 January 2017, respectively. To distinguish these two transitions, the former is marked as Case-2A and the latter is Case-2B. Table 2 compares the values of mean and standard deviation of different variables between CSs and TSs. Generally, the mean concentration of $PM_{2.5}$ during the CS is much higher than that for the TS. For Case-1, wind at lower levels mainly comes from the north during the CS, while the dominant wind direction turns into south-east when it comes to the TS. However, there is no steady wind direction for Case-2.

In terms of temperature, it goes through gradual increase over CSs despite of its diurnal change, which can be attributed to two possible reasons. On one hand, the accumulation of air pollutants results in the increase of the optical depth of the atmospheric column. The majority of incoming solar radiation during the daytime is absorbed by the upper air or scattered into different direction. The part of absorbed radiation heats the upper atmospheric layer, thus contributing positively to inversion layer which is helpful to suppress the turbulent mixing in the ABL (Petäjä et al., 2016). On the other hand, the heavily polluted ABL reduces the loss of surface longwave radiation during night, which is analogous to a cloud covered night. In this case, the heated boundary layer develops into stable stratification. Furthermore, Fig. 3 depicts the change of daily mean potential temperature profiles over the CS at 15 different heights. The $\Delta\theta$ at given height was calculated by subtracting the value of θ on the last day from that on the first day of CSs. For Case-1, $\Delta\theta$ during the CS at the lowest level (5 m) is only 5.2 K. But for the top level at 250 m, $\Delta\theta$ is relatively larger with a value of 6.8 K. This result confirms that the warming of upper layers is stronger than that of lower layers, implying an increasingly stably stratified boundary layer during polluted days. Figs. 3b and 3c for Case-2 verify this conclusion as well. Besides, an ambience with high relative humidity (RH) is favorable for the increase of $PM_{2.5}$ concentration in the ABL through secondary formation by heterogeneous reactions (Quan et al., 2015; Wang et al., 2012; Faust et al., 2017) and hygroscopic growth (Engelhart et al., 2011; Petters and Kreidenweis, 2008). For Case-1, the RH during the CS keeps high with a mean value of 53% but sharply falls into a very low level once entering the TS. Similar results can be found in Case-2.

During CSs, both horizontal wind and vertical wind are weak, implying unfavorable transport conditions. On the contrary, the strength of horizontal and vertical wind notably increases during TSs. These results are consistent with that of u_*, showing a total vertical momentum flux with a mean of 0.25 m s^{-1} during the CS of Case-1 (0.19 and 0.29 m s^{-1} for Case-2). While the values of u_* are generally larger than 0.30 m s^{-1} in the TS of both two cases. According to the classic TKE budget equation (Eq. 5.2.3 in Stull, 1988), the TKE is distinctively produced by the mechanical wind shear near the surface in the TS, resulting in strong turbulent mixing in the ABL, thus more effective transport of air pollutants. Another important term in the TKE budget equation is the buoyant production or consumption. The stability parameter z/L is used here to quantify the stratification of layers near the surface. Although the values of z/L are negative during the daytime, nocturnal z/L during the CS is notably larger than 1, which means that the consumption caused by buoyancy is dominant compared with the weak production by wind shear. The strongly stable stratification near the surface restrains the vertical turbulence mixing. The reduced mixing, together with emissions and production of secondary pollutants, result in a heavily polluted layer near the surface.

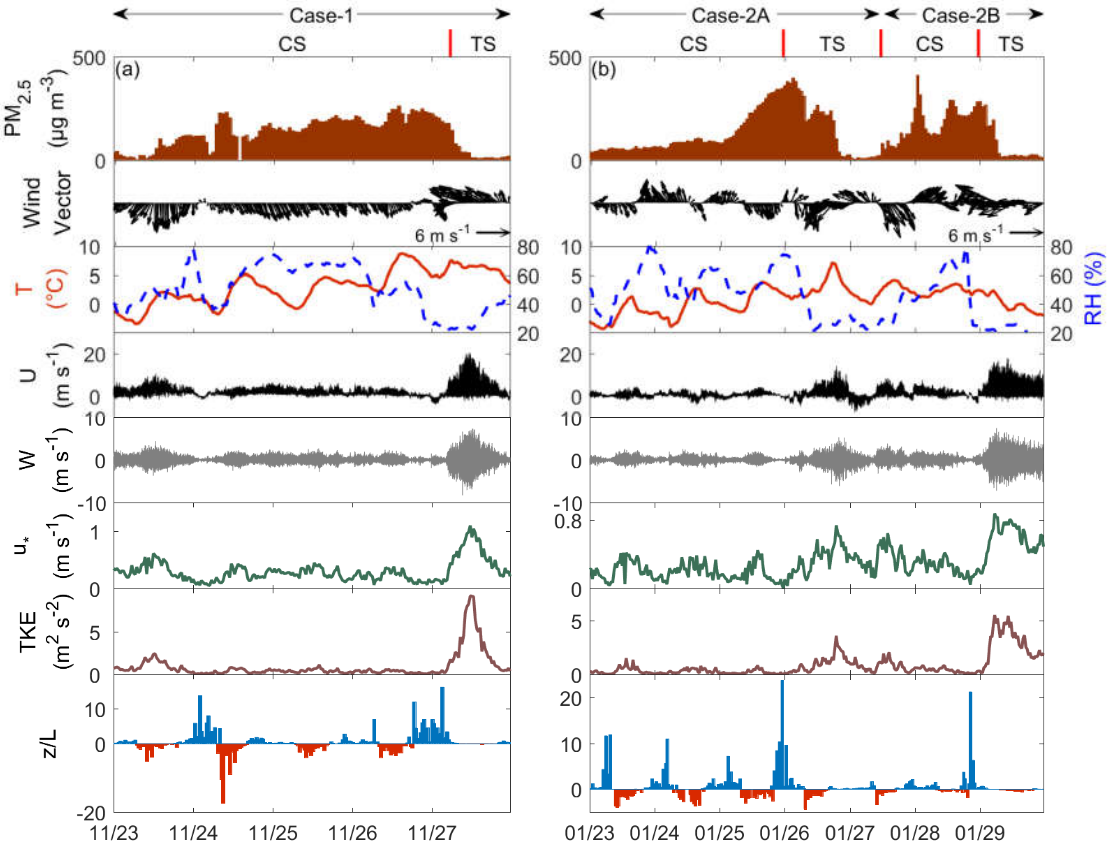

Figure 2. Time series of surface PM2.5, wind vector, temperature (T), relative humidity (RH), horizontal wind speed (U), vertical wind speed (W), friction velocity (u_*), turbulent kinetic energy (TKE), and stability parameter (z/L) for Case-1 in (a); for Case-2 in (b). The CS refers to the stage during which pollutants culminated and the TS represents clear days. All of the variables were observed at 40 m except for PM2.5 concentration which is at the surface.

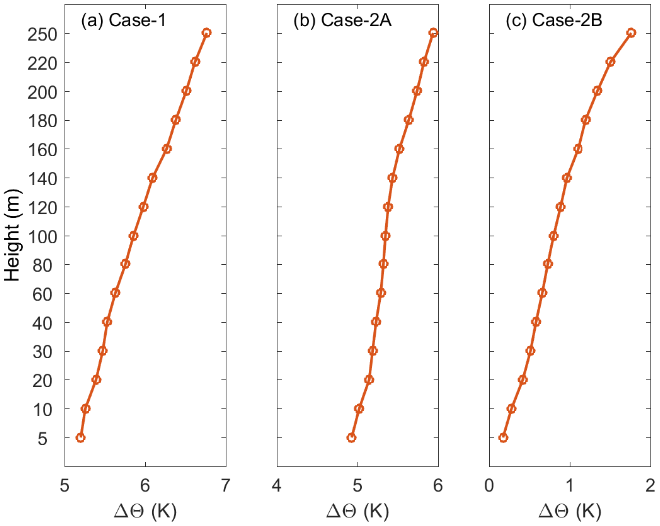

Figure 3. Vertical distribution of the change of daily mean potential temperature during CSs. Three panels refer to (a) Case-1, (b) Case-2A, and (c) Case-2B.

Table 2. Mean and standard deviation (Mean ± SD) of key variables during different periods

Variables	CS	TS	CS	TS
	Case-1		Case-2	
$PM_{2.5}$ (μg m^{-3})	145 ± 71	31 ± 35	139 ± 101 179 ± 85	104 ± 138 75 ± 92
Temperature (K)	275.6 ± 2.9	279.2 ± 0.9	272.7 ± 2.3 275.6 ± 0.8	275.4 ± 1.8 273.1 ± 1.4
RH (%)	53 ± 15	32 ± 8	54 ± 12 48 ± 15	35 ± 17 22 ± 2
U (m s^{-1})	1.85 ± 1.38	3.78 ± 2.90	0.61 ± 0.87 0.67 ± 2.03	1.47 ± 1.39 3.23 ± 1.98
Magnitude of W (m s^{-1})	0.28 ± 0.26	0.61 ± 0.64	0.23 ± 0.22 0.29 ± 0.29	0.36± 0.35 0.62 ± 0.58
u_* (m s^{-1})	0.25 ± 0.12	0.59 ± 0.26	0.19 ± 0.10 0.29 ± 0.13	0.33 ± 0.15 0.58 ± 0.18
TKE (m^2 s^{-2})	0.50 ± 0.43	3.35 ± 2.81	0.28 ± 0.93 0.25 ± 0.71	0.54 ± 0.42 2.87 ± 1.50
z/L at night	1.70 ± 2.74	0.23 ± 0.21	2.18 ± 3.74 1.36 ± 3.31	0.61 ± 1.43 0.15 ± 0.21

© Author(s) 2018. CC BY 4.0 License.

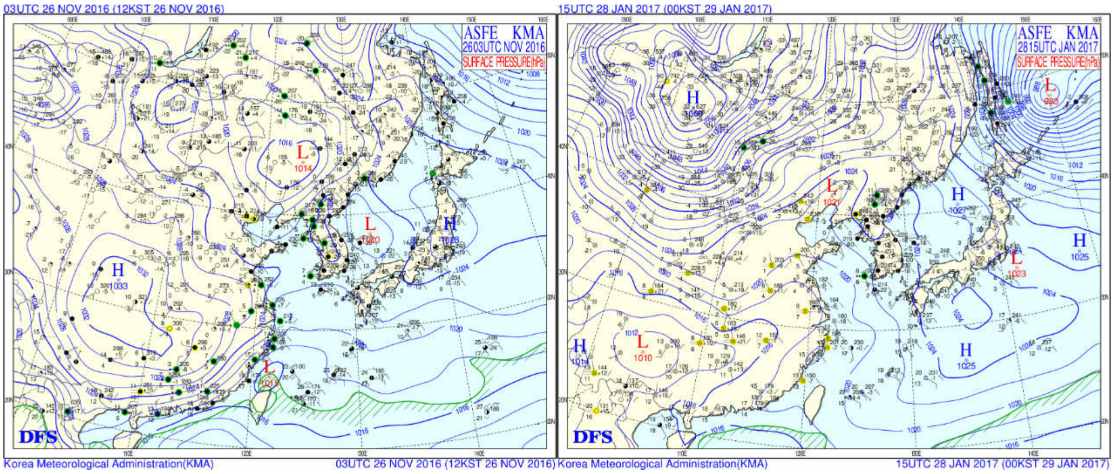

Figure 4. Typical surface weather condition during CSs. Weather charts are from Korea Meteorological Administration.

In addition to the meteorological parameters, synoptic weather conditions also play an important role in the formation and dissipation of heavy air pollutions (Zheng et al., 2015a). Fig. 4 takes two examples from Case-1 and Case-2 to illustrate the typical synoptic weather condition during CSs. In general, the accumulation of pollutants is accompanied by a low pressure system dominating the northern China. Under the control of cyclone system, this region is covered by sparse isobars and is controlled by stagnant wind field, resulting in unfavorable diffusion conditions.

3.2 Characteristics of intermittent turbulence

Considering the nonlinear and non-stationary nature of turbulent intermittency, it is imperative to choose an effective and reliable method before we implement the analyses. The arbitrary-order HSA used in this work to identify IF index meets the necessary conditions for the analyses of nonlinear and non-stationary time series, such as complete, orthogonal, local, and adaptive (Huang et al., 1998). Our previous works (Wei et al., 2016, 2017) have confirmed the validity of arbitrary-order HSA method in the identification of turbulent intermittency in the ABL.

As mentioned in Sect. 2.2, if turbulence in the ABL is fully developed, the Hilbert-based exponent scaling function $\xi(q)$ should follow the linear distribution of $\xi(q) - 1 = q/3$ (Huang et al., 2008). However, in the real world, there exit all kinds of instability mechanisms on different scales, such as the large-scale baroclinic instability and the small-scale convective instability (Frisch, 1980). Furthermore, under stable conditions, the very low boundary-layer height limit the development of eddies and the stagnant wind near the surface is not enough to maintain the turbulence mixing. Any of these mechanisms would destroy the statistical symmetries stored in the fully developed turbulence, resulting in deviations from K41's $q/3$ and a set of concave curves. Figs. 5a–5d present the behavior of $\xi(q) - 1$ at 40 m during different stages from two cases.

Compared with the theoretical $q/3$, $\xi(q)-1$ from CSs and TSs both shows deviations to some extent. However, the difference for CSs is much more obvious, indicating stronger intermittency in the turbulence. Fig. 5e further gives a two-hour example of vertical wind speed during 23:00 on 25 January to 01:00 and 26 January 2017, which covers the transition from the CS to TS in Case-2A. One noticeable feature is that the magnitude of vertical wind fluctuation significantly increases and is marked by strong burst lasting for nearly 25 min from 00:20 to 00:45 on 26 January 2017. On the contrary, the vertical wind speed is relatively weak and steady during the CS. But it should be kept in mind that the small deviations during CSs do not manifest fully developed turbulence but result from the very weak wind speed in the ABL, at which point the wind shear is either absent or not strong enough to generate intermittency (Van de Wiel et al., 2003). The magnitude of vertical wind speed for CSs is generally less than 0.58 m s^{-1}. Under extremely stable conditions, the size of eddies may be too small to be detected by sonic anemometers (Mahrt, 2014).

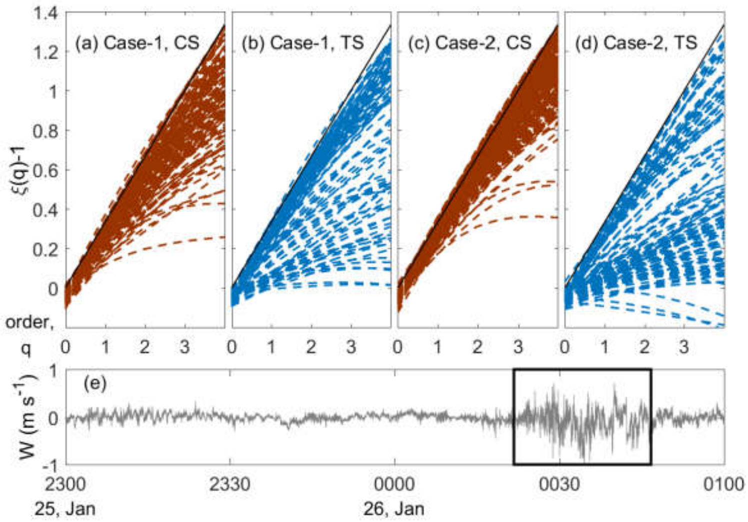

Figure 5. Hilbert-based scaling exponent function at 40 m during different stages for (a) – (b) Case-1 and (c) – (d) Case-2, where the black line denotes the K41 result $q/3$. (e) compares vertical wind fluctuation at 40 m between the CS (before 00:00 on 26 January 2017) and TS (after 00:00 on 26 January 2017). The latter shows apparent 'bursts' marked by the rectangular frame.

In order to measure the strength of turbulent intermittency at different levels, an index named as IF was proposed by this work. Since IF is defined as the deviation from the theoretical $q/3$ at the maximal order q_{max} (here q_{max} equal to 4, see Sect. 2.2), the larger absolute values of IF indicate stronger turbulent intermittency at given height. Meanwhile, time with magnitude of vertical wind speed at 40 m less than 0.3 m s^{-1} is marked to exclude stagnant wind. Fig. 6 illustrates the distribution of IF at three levels, compared with the concentration of $PM_{2.5}$ at the surface. Each sharp decline of surface $PM_{2.5}$ concentration is accompanied by the abrupt change in values of IF. And IF at 40 m level is especially in agreement with the accumulation and dissipation of pollutants at the surface. The increasing deviations of IF when entering the TS manifest more intermittent turbulence, thus stronger vertical mixing in the ABL. Previous field site results indicate that a

© Author(s) 2018. CC BY 4.0 License.

significant proportion of vertical fluxes of heat, momentum, and mass under stable conditions come from intermittent bursts (Poulos et al., 2002). The enhanced turbulent mixing caused by intermittent bursts contributes positively to the vertical transport of pollutants, improving the air quality near the surface.

Besides, another feature of IF in Fig. 6 is that the occurrence of abruptly changed IF at different heights is not simultaneous. In general, the higher the level is, the earlier the intermittent turbulence happens and also the greater the deviations of IF are, which implies that the intermittent turbulence is generated at higher levels and then transported downward. We know that, under weakly stable conditions, turbulence in the ABL is continuous in both time and space, which is mainly dominated by wind shear at the surface. But for strongly stable cases, buoyancy prohibits the turbulent mixing, which enhances the surface radiative cooling, thus increasing the stratification of the ABL (Derbyshire, 1999). Such a positive feedback ultimately leads to the decoupling of boundary layer from the underlying surface, that is, the strong stratification prevents the turbulent exchange between the surface and the ABL. This decoupling could be ceased if there exists wind shear above the stable surface layer, at which point turbulence may be generated at upper levels and then transported downward to rebuild the coupling between the atmosphere and the surface (Mahrt, 1999). The decoupling is suddenly interrupted by the descending turbulence, resulting in intermittent bursts near the surface (Van de Wiel et al., 2012). It is reported (Smedman et al., 1995) that this downward transport of turbulence is related to the pressure transport term in the TKE equation, which means that Monin-Obukhov similarity theory is invalid for this case.

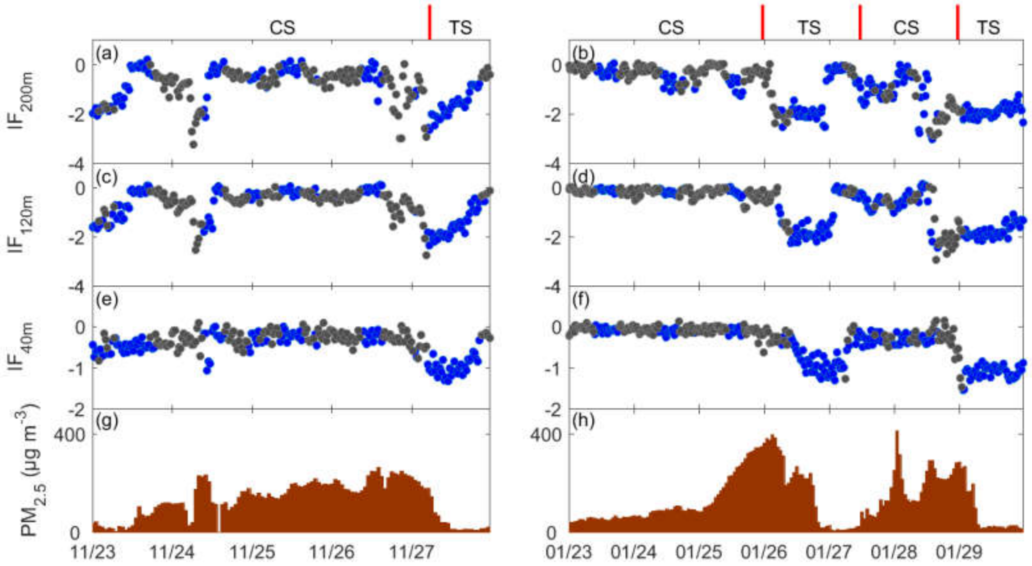

Figure 6. Distribution of (a) – (f) IF at three levels and (g) – (h) concentration of PM2.5 at the surface. Left panel represents Case-1 and right panel for Case-2. Grey dots denote stagnant wind with vertical wind speed less than 0.3 m s^{-1}.

© Author(s) 2018. CC BY 4.0 License.

3.3 Mechanism and transport of intermittency

The reasons for intermittent turbulence under stable conditions have not yet been well understood. Some potential causes include gravity waves (Sorbjan and Czerwinska, 2013; Strang and Fernado, 2001), solitary waves (Terradellas et al., 2005), horizontal meandering of the mean wind field (Anfossi et al., 2005), and low-level jets (LLJs, Marht, 2014).

According to the case overview in Sect. 3.1, it can be seen that the stratification of surface layers at night is fairly stable during CSs with values of $z/L \gg 1$. Meanwhile, weak u_* and TKE favor the accumulation of pollutants near the surface. In the case of decoupling, it is hard to generate turbulence through the interaction between the atmosphere and the surface. To detect the main sources of turbulence, Fig. 7 presents the height–time cross-section of horizontal wind speed under 2,000 m. The lowest height range of WPR is at 200 m below which observations are seriously interfered by the hard-target returns of around buildings or trees. From Fig. 7a, strong wind occurs at night of 26 November 2016 with maximal wind speed larger than 15 m s^{-1}. For Case-2, there is also strong wind happening in the ABL right before the transitions between the CS and TS (Fig. 7b). After detecting the horizontal wind field, we found that the strong wind in the ABL is generally associated with the happening of LLJs. Fig. 8 takes three profiles as examples to illustrate the LLJ in the ABL. The vertical 'nose' shape of LLJs provides wind shear at upper levels, working as an elevated source of turbulent mixing. Then this turbulence is transported downward to the surface, resulting in non-stationary increase of turbulent mixing at lower levels. The differences in phase and strength of intermittency at three levels in Fig. 6 indicate that the wind shear associated with the LLJ 'nose' may play an important part in the generation and transport of turbulence in the ABL. Previous study (Wei et al., 2014) has revealed that the LLJ is a common phenomenon in Tianjin region, due to the combined effects of plain terrain for inertial oscillation (Lundquist, 2003) and strong baroclinicity related to the land–sea temperature contrast offshore (Parish, 2000). In addition, the reduced convection in winter is helpful to maintain the LLJs even during the daytime. In a word, the frequent LLJs in Tianjin region may be a key factor to understand the mechanisms of intermittent turbulence.

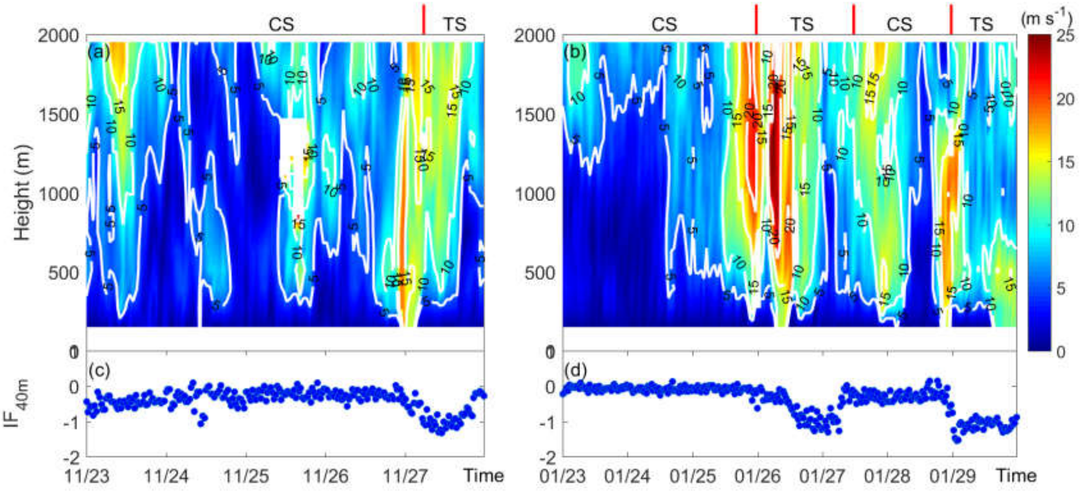

© Author(s) 2018. CC BY 4.0 License.

Figure 7. Height–time cross-section of horizontal wind speed observed by WPR for (a) Case-1 and (b) Case-2. (c) – (d) present the corresponding IF at 40 m.

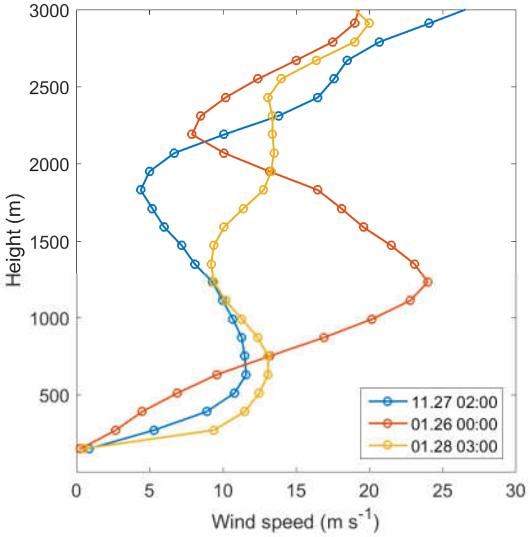

Figure 8. Sample LLJ profiles for three transitions between CSs and TSs.

Finally, we summary the mechanism of intermittent turbulence affecting the $PM_{2.5}$ concentration near the surface in a schematic figure in Fig. 9. In the beginning, the inversion layer near the surface enhances due to some favorable conditions including steady synoptic systems, stagnant wind, high temperature and high RH, which leads to the gradual accumulation of particles in the lower boundary layer. Such a process is named as the cumulative stage or CS, during which the turbulence near the surface is too weak to transport pollutants upward. In this case, if there existed LLJs (or other motions) in the ABL, the turbulence could be generated by the strong wind shear associated with the LLJs and then transport downward, resulting in intermittent turbulence at lower levels. The suddenly increased vertical mixing is helpful for the abrupt dissipation of $PM_{2.5}$ near the surface.

© Author(s) 2018. CC BY 4.0 License.

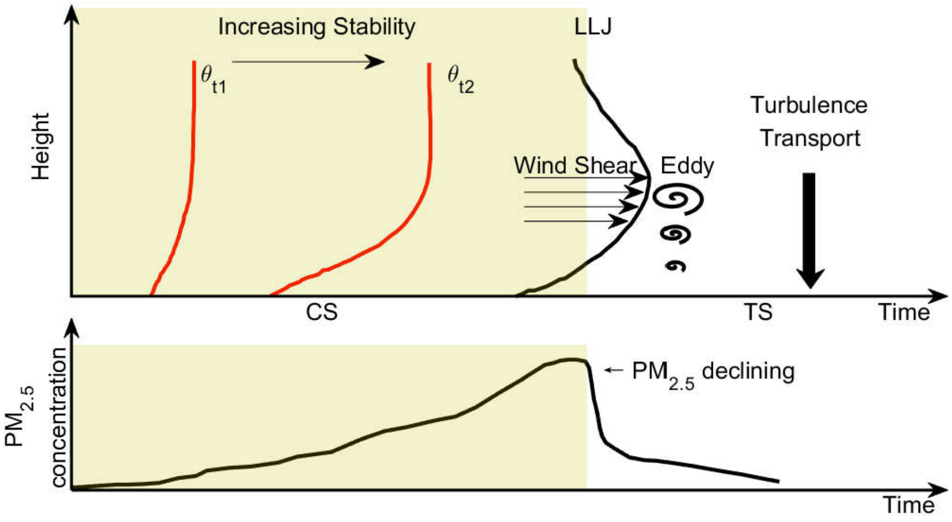

Figure 9. Schematic of how intermittent turbulence affects the dissipation of PM2.5 near the surface.

4 Conclusion

In the winter of 2016–2017, severe air pollution events haunted the North China Plain. Extremely high concentration of $PM_{2.5}$ threatens the health of the large population living in this region. In this work, two cases in Tianjin (39.00°N, 117.43°E), China were drawn upon to study the effects of intermittent turbulence on the improvement of air quality near the surface. Observations from a 255-m tower, a CFL-03 WPR and a TEOM 1405-DF system were analyzed to investigate the features of boundary-layer structure and $PM_{2.5}$ concentration. In order to measure the levels of turbulent intermittency, an index called intermittent factor (IF) was proposed based on the arbitrary-order HSA which is more suitable for the analyses of nonlinear and non-stationary signals.

At first, due to the absorbed solar radiation by upper air pollutants and the reduced loss of surface longwave outgoing radiation, the inversion layer enhances with stronger heating of upper air layers. The stability function z/L keeps at high values (>> 1) at night and the stagnant wind field impedes the transport of pollutants. Additionally, high RH and steady cyclone system further aggravate the air pollution. All these factors result in the accumulation of pollutants near the surface.

On the other hand, the concentration of $PM_{2.5}$ undergoes rapid decrease during the dissipation periods, dropping from more than 250 μg m^{-3} to less than 50 μg m^{-3} within a few hours. The dispersion of pollutants coincides with the enhanced turbulent mixing in the ABL. The mean values of u_* and TKE rise to 2–9 times those of the polluted periods. The Hilbert-based exponent scaling function $\xi(q)$ shows great deviations from K41's theoretical result of $q/3$ by a set of concave curves, indicating that the enhanced turbulence in the ABL is intermittent rather than continuous or fully developed. Using the IF index derived from the vertical wind speed, the abrupt change in IF at 40 m is in agreement with the sharp drop of $PM_{2.5}$ concentration. In addition, the occurrence and strength of intermittent turbulence differ with observation levels. In short, the higher the level is, the earlier the turbulence happens and the stronger the intermittency is, which implies that turbulence is mainly generated at upper levels and then transported to the surface.

From the observation of WPR, LLJs were detected right before the dispersion of $PM_{2.5}$. Previous work (Marht, 2014) has pointed out that the stronger wind shear at the height of LLJ 'nose' can be a source of turbulence under the condition of decoupling between the atmosphere and the surface. In this work, LLJs play a key role in the generation of upper-level turbulence. The subsequent downward transport of turbulence leads to intermittent mixing near the surface, thus enhancing the vertical dispersion of $PM_{2.5}$ and improving the air quality.

Data availability. Data used in this study are available from the corresponding author upon request (hsdq@pku.edu.cn).

Competing interests. The authors declare that they have no conflict of interest.

Acknowledgement. This work was jointly funded by grant from National Key R&D Program of China (2016YFC0203300), the National Natural Science Foundation of China (91544216, 41705003, 41475007, 41675018). We also thank Dr. Gao Shanhong at Ocean University of China for providing historical weather-condition charts. Many thanks to Sr. Engr. Yao Qing and Liu Jinle at Tianjin Municipal Meteorological Bureau for their help with the data observation.

References

Anfossi, D., Oettl, D., Degrazia, G. and Goulart, A.: An analysis of sonic anemometer observations in low wind speed conditions, Boundary-Layer Meteorol., 114(1), 179–203, doi:10.1007/s10546-004-1984-4, 2005.

Banta, R. M., Pichugina, Y. L. and Brewer, W. A.: Turbulent Velocity-Variance Profiles in the Stable Boundary Layer Generated by a Nocturnal Low-Level Jet, J. Atmos. Sci., 63(11), 2700–2719, doi:10.1175/JAS3776.1, 2006.

Basu, S., Foufoula-Georgiou, E. and Porté-Agel, F.: Synthetic turbulence, fractal interpolation, and large-eddy simulation, Phys. Rev. E, 70(2), 26310, doi:10.1103/PhysRevE.70.026310, 2004.

Bressi, M., Sciare, J., Ghersi, V., Bonnaire, N., Nicolas, J. B., Petit, J. E., Moukhtar, S., Rosso, A., Mihalopoulos, N. and Féron, A.: A one-year comprehensive chemical characterisation of fine aerosol (PM2.5) at urban, suburban and rural background sites in the region of Paris (France), Atmos. Chem. Phys., 13(15), 7825–7844, doi:10.5194/acp-13-7825-2013, 2013.

Cohen, L.: Time-frequency analysis, Prentice Hall, Englewood Cliffs, NJ, 1995.

Derbyshire, S. H.: Boundary-layer decoupling over cold surfaces as a physical boundary-instability, Boundary-Layer Meteorol., 90(2), 297–325, doi:10.1023/A:1001710014316, 1999.

Dominici, F., Greenstone, M. and Sunstein, C. R.: Particulate Matter Matters, Science, 344(6181), 257–259, doi: 10.1126/science.1247348, 2014.

Engelhart, G. J., Hildebrandt, L., Kostenidou, E., Mihalopoulos, N., Donahue, N. M. and Pandis, S. N.: Water content of aged aerosol, Atmos. Chem. Phys., 11(3), 911–920, doi:10.5194/acp-11-911-2011, 2011.

Faust, J. A., Wong, J. P. S., Lee, A. K. Y., and Abbatt, J. P.: Role of Aerosol Liquid Water in Secondary Organic Aerosol Formation from Volatile Organic Compounds, Environ. Sci. Techmol., 51(3): 1405-1413, doi: 10.1021/acs.est.6b04700, 2017.

Frisch, U.: Fully developed turbulence and intermittency, Ann. NY. Acad. Sci., 357(1): 359-367, doi: 10.1111/j.1749-6632.1980.tb29703.x, 1980.

Frisch, U.: Turbulence: the legacy of AN Kolmogorov, Cambridge university press, Great Britain, 1995.

Gao, S., Wang, Y., Huang, Y., Zhou, Q., Lu, Z., Shi, X. and Liu, Y.: Spatial statistics of atmospheric particulate matter in China, Atmos. Environ., 134, 162–167, doi:10.1016/j.atmosenv.2016.03.052, 2016.

Helgason, W. and Pomeroy, J. W.: Characteristics of the near-surface boundary layer within a mountain valley during winter, J. Appl. Meteorol. Climatol., 51(3), 583–597, doi:10.1175/JAMC-D-11-058.1, 2012.

Holtslag, A. A. M.: BOUNDARY LAYER (ATMOSPHERIC) AND AIR POLLUTION | Modeling and Parameterization, in Encyclopedia of Atmospheric Sciences, vol. 1, pp. 265–273, Elsevier., 2015.

Huang, N., Shen, Z., Long, S., Wu, M., Shih, H., Zheng, Q., Yen, N., Tung, C. and Liu, H.: The empirical mode decomposition and the Hilbert spectrum for nonlinear and non-stationary time series analysis, Proc. R. Soc. A Math. Phys. Eng. Sci., 454(1971), 903–995, doi:10.1098/rspa.1998.0193, 1998.

Huang, N. E., Shen, Z. and Long, S. R.: A new view of nonlinear water waves: the Hilbert Spectrum, Annu. Rev. Fluid Mech., 31(1), 417–457, doi:10.1146/annurev.fluid.31.1.417, 1999.

Huang, Y., Schmitt, F. G., Lu, Z. and Liu, Y.: Analysis of daily river flow fluctuations using empirical mode decomposition and arbitrary order Hilbert spectral analysis, J. Hydrol., 373(1–2), 103–111, doi:10.1016/j.jhydrol.2009.04.015, 2009.

Huang, Y. X., Schmitt, F. G., Lu, Z. M. and Liu, Y. L.: An amplitude-frequency study of turbulent scaling intermittency using Empirical Mode Decomposition and Hilbert Spectral Analysis, EPL (Europhysics Lett., 84(4), 40010, doi:10.1209/0295-5075/84/40010, 2008.

Huang, Y. X., Schmitt, F. G., Hermand, J. P., Gagne, Y., Lu, Z. M. and Liu, Y. L.: Arbitrary-order Hilbert spectral analysis for time series possessing scaling statistics: Comparison study with detrended fluctuation analysis and wavelet leaders, Phys. Rev. E, 84(1), 16208, doi:10.1103/PhysRevE.84.016208, 2011.

Klipp, C. L. and Mahrt, L.: Flux-gradient relationship, self-correlation and intermittency in the stable boundary layer, Q. J. R. Meteorol. Soc., 130(601), 2087–2103, doi:10.1256/qj.03.161, 2004.

Lundquist, J. K.: Intermittent and Elliptical Inertial Oscillations in the Atmospheric Boundary Layer, J. Atmos. Sci., 60(1997), 2661–2673, doi:10.1175/1520-0469(2003)060<2661:IAEIOI>2.0.CO;2, 2003.

Mahrt, L.: Nocturnal Boundary-Layer Regimes, Boundary-layer Meteorol., 88(2), 255–278, doi:10.1023/A:1001171313493, 1998.

Mahrt, L.: Stratified Atmospheric Boundary Layers, Boundary-Layer Meteorol., 90(3), 375–396, doi:10.1023/A:1001765727956, 1999.

Mahrt, L.: Stably Stratified Atmospheric Boundary Layers, Annu. Rev. Fluid Mech., 46, 23–45, doi:10.1146/annurev-fluid-010313-141354, 2014.

Miao, Y., Guo, J., Liu, S., Liu, H., Zhang, G., Yan, Y. and He, J.: Relay transport of aerosols to Beijing-Tianjin-Hebei region by multi-scale atmospheric circulations, Atmos. Environ., 165, 35–45, doi:10.1016/j.atmosenv.2017.06.032, 2017.

Nel, A.: ATMOSPHERE: Enhanced: Air Pollution-Related Illness: Effects of Particles, Science, 308(5723), 804–806, doi:10.1126/science.1108752, 2005.

Noone, D., Risi, C., Bailey, A., Berkelhammer, M., Brown, D. P., Buenning, N., Gregory, S., Nusbaumer, J., Schneider, D., Sykes, J., Vanderwende, B., Wong, J., Meillier, Y. and Wolfe, D.: Determining water sources in the boundary layer from tall tower profiles of water vapor and surface water isotope ratios after a snowstorm in Colorado, Atmos. Chem. Phys., 13(3), 1607–1623, doi:10.5194/acp-13-1607-2013, 2013.

Parish, T. R.: Forcing of the Summertime Low-Level Jet along the California Coast, J. Appl. Meteorol., 39(12), 2421–2433, doi:10.1175/1520-0450(2000)039<2421:FOTSLL>2.0.CO;2, 2000.

Petäjä, T., Järvi, L., Kerminen, V. M., Ding, A. J., Sun, J. N., Nie, W., Kujansuu, J., Virkkula, A., Yang, X., Fu, C. B., Zilitinkevich, S. and Kulmala, M.: Enhanced air pollution via aerosol-boundary layer feedback in China, Sci. Rep., 6(January), doi:10.1038/srep18998, 2016.

Petters, M. D. and Kreidenweis, S. M.: A single parameter representation of hygroscopic growth and cloud condensation nucleus activity &ndash; Part 2: Including solubility, Atmos. Chem. Phys. Discuss., 8(2), 5939–5955, doi:10.5194/acpd-8-5939-2008, 2008.

Poulos, G. S., Blumen, W., Fritts, D. C., Lundquist, J. K., Sun, J., Burns, S. P., Nappo, C., Banta, R., Newsom, R., Cuxart, J., Terradellas, E., Balsley, B. and Jensen, M.: CASES-99: A comprehensive investigation of the stable nocturnal boundary layer, Bull. Am. Meteorol. Soc., 83(4), 555–581, doi:10.1175/1520-0477(2002)083<0555:CACIOT>2.3.CO;2, 2002.

Quan, J., Liu, Q., Li, X., Gao, Y., Jia, X., Sheng, J. and Liu, Y.: Effect of heterogeneous aqueous reactions on the secondary formation of inorganic aerosols during haze events, Atmos. Environ., 122, 306–312, doi:10.1016/j.atmosenv.2015.09.068, 2015.

Ren, Y., Zheng, S., Wei, W., Wu, B., Zhang, H., Cai, X. and Song, Y.: Characteristics of the Turbulent Transfer during the Heavy Haze in Winter 2016 / 17 in Beijing, J. Meteorol. Res., doi:10.1007/s13351-018-7072-3, 2017.

Salmond, J. A.: Wavelet analysis of intermittent turbulence in a very stable nocturnal boundary layer: implications for the vertical mixing of ozone, Boundary-Layer Meteorol., 114(3), 463–488, doi:10.1007/s10546-004-2422-3, 2005.

© Author(s) 2018. CC BY 4.0 License.

Schmitt, F. G., Huang, Y., Lu, Z., Liu, Y. and Fernandez, N.: Analysis of velocity fluctuations and their intermittency properties in the surf zone using empirical mode decomposition, J. Mar. Syst., 77(4), 473–481, doi:10.1016/j.jmarsys.2008.11.012, 2009.

Shen, Z., Cui, G. and Zhang, Z.: Turbulent dispersion of pollutants in urban-type canopies under stable stratification conditions, Atmos. Environ., 156, 1–14, doi:10.1016/j.atmosenv.2017.02.017, 2017.

Smedman, A. S., Bergström, H. and Högström, U.: Spectra, variances and length scales in a marine stable boundary layer dominated by a low level jet, Boundary-Layer Meteorol., 76(3), 211–232, doi:10.1007/BF00709352, 1995.

Sorbjan, Z. and Czerwinska, A.: Statistics of Turbulence in the Stable Boundary Layer Affected by Gravity Waves, Boundary-Layer Meteorol., 148(1), 73–91, doi:10.1007/s10546-013-9809-y, 2013.

Strang, E. J. and Fernado, H. J. S.: Entrainment and mixing in stratified shear flows, J. Fluid Mech., 428(6S), 349–386, doi:10.1017/S0022112000002706, 2001.

Stull, R.B.: An Introduction to Boundary Layer Meteorology, Kluwer Academic, USA, 1988.

Sun, J., Mahrt, L., Nappo, C. and Lenschow, D. H.: Wind and Temperature Oscillations Generated by Wave–Turbulence Interactions in the Stably Stratified Boundary Layer, J. Atmos. Sci., 72(4), 1484–1503, doi:10.1175/JAS-D-14-0129.1, 2015.

Sun, Y., Zhuang, G., Wang, Y., Han, L., Guo, J., Dan, M., Zhang, W., Wang, Z. and Hao, Z.: The air-borne particulate pollution in Beijing - Concentration, composition, distribution and sources, Atmos. Environ., 38(35), 5991–6004, doi:10.1016/j.atmosenv.2004.07.009, 2004.

Tang, G., Zhang, J., Zhu, X., Song, T., Münkel, C., Hu, B., Schäfer, K., Liu, Z., Zhang, J., Wang, L., Xin, J., Suppan, P. and Wang, Y.: Mixing layer height and its implications for air pollution over Beijing, China, Atmos. Chem. Phys., 16(4), 2459–2475, doi:10.5194/acp-16-2459-2016, 2016.

Terradellas, E., Soler, M. R., Ferreres, E. and Bravo, M.: Analysis of oscillations in the stable atmospheric boundary layer using wavelet methods, Boundary-Layer Meteorol., 114, 489–518, doi:10.1007/s10546-004-1293-y, 2005.

Thompson, T. M., Saari, R. K. and Selin, N. E.: Air quality resolution for health impact assessment: Influence of regional characteristics, Atmos. Chem. Phys., 14(2), 969–978, doi:10.5194/acp-14-969-2014, 2014.

Vindel, J. M. and Yagüe, C.: Intermittency of Turbulence in the Atmospheric Boundary Layer: Scaling Exponents and Stratification Influence, Boundary-Layer Meteorol., 140(1), 73–85, doi:10.1007/s10546-011-9597-1, 2011.

Wang, T., Nie, W., Gao, J., Xue, L. K., Gao, X. M., Wang, X. F., Qiu, J., Poon, C. N., Meinardi, S., Blake, D., Wang, S. L., Ding, A. J., Chai, F. H., Zhang, Q. Z. and Wang, W. X.: Air quality during the 2008 Beijing Olympics: Secondary pollutants and regional impact, Atmos. Chem. Phys., 10(16), 7603–7615, doi:10.5194/acp-10-7603-2010, 2010.

Wang, X., Wang, W., Yang, L., Gao, X., Nie, W., Yu, Y., Xu, P., Zhou, Y. and Wang, Z.: The secondary formation of inorganic aerosols in the droplet mode through heterogeneous aqueous reactions under haze conditions, Atmos. Environ., 63, 68–76, doi:10.1016/j.atmosenv.2012.09.029, 2012.

Wang, X., Dickinson, R. E., Su, L., Zhou, C. and Wang, K.: PM 2.5 Pollution in China and How It Has Been Exacerbated by Terrain and Meteorological Conditions, Bull. Am. Meteorol. Soc., doi:10.1175/BAMS-D-16-0301.1, 2017.

© Author(s) 2018. CC BY 4.0 License.

Wei, W., Zhang, H. S. and Ye, X. X.: Comparison of low-level jets along the north coast of China in summer, J. Geophys. Res. Atmos., 119(16), 9692–9706, doi:10.1002/2014JD021476, 2014.

Wei, W., Schmitt, F. G., Huang, Y. X. and Zhang, H. S.: The Analyses of Turbulence Characteristics in the Atmospheric Surface Layer Using Arbitrary-Order Hilbert Spectra, Boundary-Layer Meteorol., 159(2), 391–406, doi:10.1007/s10546-015-0122-9, 2016.

Wei, W., Wang, M., Zhang, H., He, Q., Ali, M. and Wang, Y.: Diurnal characteristics of turbulent intermittency in the Taklimakan Desert, Meteorol. Atmos. Phys., doi:10.1007/s00703-017-0572-3, 2017.

Van de Wiel, B. J. H., Moene, a. F., Hartogensis, O. K., De Bruin, H. a. R. and Holtslag, a. a. M.: Intermittent Turbulence in the Stable Boundary Layer over Land. Part III: A Classification for Observations during CASES-99, J. Atmos. Sci., 60(20), 2509–2522, doi:10.1175/1520-0469(2003)060<2509:ITITSB>2.0.CO;2, 2003.

Van de Wiel, B. J. H., Moene, A. F., Jonker, H. J. J., Baas, P., Basu, S., Donda, J. M. M., Sun, J. and Holtslag, A. A. M.: The Minimum Wind Speed for Sustainable Turbulence in the Nocturnal Boundary Layer, J. Atmos. Sci., 69(11), 3116–3127, doi:10.1175/JAS-D-12-0107.1, 2012.

Ye, X., Wu, B. and Zhang, H.: The turbulent structure and transport in fog layers observed over the Tianjin area, Atmos. Res., 153, 217–234, doi:10.1016/j.atmosres.2014.08.003, 2014.

Ye, X., Song, Y., Cai, X. and Zhang, H.: Study on the synoptic flow patterns and boundary layer process of the severe haze events over the North China Plain in January 2013, Atmos. Environ., 124(January 2013), 129–145, doi:10.1016/j.atmosenv.2015.06.011, 2016.

Yin, Z. and Wang, H.: Role of atmospheric circulations in haze pollution in December 2016, Atmos. Chem. Phys., 17(18), 11673–11681, doi:10.5194/acp-17-11673-2017, 2017.

Yin, Z., Wang, H. and Chen, H.: Understanding severe winter haze events in the North China Plain in 2014: Roles of climate anomalies, Atmos. Chem. Phys., 17(3), 1641–1651, doi:10.5194/acp-17-1641-2017, 2017.

Zhang, H., Chen, J. and Park, S.: Turbulence structure in unstable conditions over various surfaces, Boundary-Layer Meteorol., 100(2), 243–261, doi:10.1023/A:1019223316895, 2001.

Zhang, H., Wang, S., Hao, J., Wang, X., Wang, S., Chai, F. and Li, M.: Air pollution and control action in Beijing, J. Clean. Prod., 112, 1519–1527, doi:10.1016/j.jclepro.2015.04.092, 2016.

Zhang, J. P., Zhu, T., Zhang, Q. H., Li, C. C., Shu, H. L., Ying, Y., Dai, Z. P., Wang, X., Liu, X. Y., Liang, A. M., Shen, H. X. and Yi, B. Q.: The impact of circulation patterns on regional transport pathways and air quality over Beijing and its surroundings, Atmos. Chem. Phys., 12(11), 5031–5053, doi:10.5194/acp-12-5031-2012, 2012.

Zhang, Y.-L. and Cao, F.: Fine particulate matter (PM2.5) in China at a city level, Sci. Rep., 5(October), 14884, doi:10.1038/srep14884, 2015.

Zheng, G. J., Duan, F. K., Su, H., Ma, Y. L., Cheng, Y., Zheng, B., Zhang, Q., Huang, T., Kimoto, T., Chang, D., Pöschl, U., Cheng, Y. F. and He, K. B.: Exploring the severe winter haze in Beijing: The impact of synoptic weather, regional transport and heterogeneous reactions, Atmos. Chem. Phys., 15(6), 2969–2983, doi:10.5194/acp-15-2969-2015, 2015a.

© Author(s) 2018. CC BY 4.0 License.

Zheng, S., Pozzer, A., Cao, C. X. and Lelieveld, J.: Long-term (2001-2012) concentrations of fine particulate matter (PM2.5) and the impact on human health in Beijing, China, Atmos. Chem. Phys., 15(10), 5715–5725, doi:10.5194/acp-15-5715-2015, 2015b.

Zhong, J., Zhang, X., Wang, Y., Sun, J., Zhang, Y., Wang, J., Tan, K., Shen, X., Che, H., Zhang, L., Zhang, Z., Qi, X., Zhao, H., Ren, S. and Li, Y.: Relative contributions of boundary-layer meteorological factors to the explosive growth of PM2.5during the red-alert heavy pollution episodes in Beijing in December 2016, J. Meteorol. Res., 31(5), 809–819, doi:10.1007/s13351-017-7088-0, 2017.